Title
Spreading of liquid Silver and Silver-Molybdenum alloys on molybdenum substrates

Journal
Zeitschrift fur Metallkunde, 94(3)

Authors
Rauch, Nicole
Saiz, Eduardo
Tomsia, Antoni P.

Publication Date
2002-08-01

Spreading of liquid silver and silver-molybdenum alloys on molybdenum substrates

Nicole Rauch, Eduardo Saiz, Antoni P. Tomsia

Materials Science Division, Lawrence Berkeley National Laboratory, Berkeley, CA 94720, USA.

Abstract

The spreading of liquid Ag and Ag-Mo alloys on molybdenum substrates has been studied using a drop-transfer setup. Even though initial spreading velocities as fast as ~1 m/s have been recorded in some experiments, a large variation in the spreading dynamics has been observed, and there is no unique relationship between the contact angle and the spreading velocity. This can be attributed to the formation of ridges at the triple junction, the movement of which controls spreading. The fastest spreading rates are consistent with results reported for low temperature liquids; these can be described using a molecular-kinetic model. Spreading kinetics and final contact angles were similar for pure silver and silver-molybdenum liquids.

Introduction

Due to its great technological importance, a large body of empirical knowledge has been accumulated on the wetting of molten metals and oxides on various substrates [1-6]. However, in most of these systems the results are ambiguous and even inconsistent, and the theoretical analysis of high-temperature wetting and spreading lags far behind the

progress made for low-temperature systems. This is in part due to the inherent complexity of high-temperature systems, for which the substrates cannot be described as rigid and insoluble, and in which spreading is usually accompanied by adsorption, triple line ridging, interdiffusion, or interfacial reactions. In addition, the experiments are challenging since they require temperature and atmosphere control. For these reasons, high-temperature wetting experiments are generally performed using a conventional sessile drop configuration, in which it is difficult both to separate the basic spreading process from additional effects (such as melting, equilibration with the atmosphere, removal of oxide layers, etc.) and to record the spreading kinetics accurately [1-4].

In this work, a drop-transfer setup combined with high speed photography has been used to analyze the spreading of Ag and Ag-Mo alloys on molybdenum substrates. The drop-transfer setup provides a unique opportunity to systematically analyze isothermal spreading, thus avoiding the complications related to melting and equilibration. The Ag-Mo system has been selected because of its simplicity. The phase diagram predicts no interfacial reactions, the mutual solubilities are very small, and the melting point of the substrate is much higher than the experimental temperature. The goal is to unveil the basic phenomena controlling spreading in metal-metal systems and to provide the basic data needed to elaborate new theories for high-temperature spreading.

Experimental

The spreading of liquid Ag and Ag-Mo alloys on Mo substrates was analyzed using a drop-transfer setup inside an induction furnace with a W heating element. The experiments were performed in Ar + 1% H_2 flowing at ~$2 \cdot 10^{-5}$ m^3/s [$p(Ar) \approx 10^5$ Pa]. The oxygen content of the gas leaving the furnace was measured using a ZrO_2 sensor (Centorr, model 2D). For all the experiments, the oxygen content in the gas was kept lower than $1 \cdot 10^{-14}$ ppm [$p(O_2) < 10^{-21}$ atm]. Prior to the experiments, the Mo substrates (~20 x 20 mm, 1 mm thick) were polished with 1 μm diamond particles. Silver-molybdenum alloys (1 atomic% Mo) were prepared by dry mixing of Ag and Mo powders, with average particle sizes of 1 μm for Mo and 2-3.5 μm for Ag, in a ball mill using teflon balls. After mixing, the powders were uniaxially pressed at 6 MPa to form cylindrical pellets (25mm diameter, 4mm height) that were then annealed in flowing H_2 at 850°C for 16h. The alloys are saturated with Mo at the experimental temperature, so the liquid is fully equilibrated with molybdenum during the experiments and no dissolution of the substrate should occur (Figure 1) [7]. The silver alloys and the substrates were cleaned with acetone and ethanol in an ultrasonic bath and dried with an air gun before the experiments.

Drop-transfer spreading experiments were performed using the following procedure. A small piece of silver or Ag-Mo (~0.1-0.2 g) was placed on an alumina or zirconia single-crystal substrate inside the furnace. The molybdenum substrate was placed on a Mo holder ~5–10 mm above the molten Ag or Ag-Mo drop. Subsequently, the furnace was

evacuated to a pressure of ~$6 \cdot 10^{-4}$ Pa and refilled with gas (Ar + 1% H_2). The gas was allowed to flow for ~2 h before heating in order to assure that the required $p(O_2)$ was reached. The assembly was heated at 25°C/min to 1000°C. When the temperature reached 1000°C, the Mo substrate was lowered from the top and placed in close proximity to the liquid surface (~1 mm or less). The assembly was maintained at 1000°C for 1 h. Afterwards, the substrate was lowered slowly until it just touched the drop surface and the liquid spread on it, transferring from the ceramic plate to the alloy (Figure 2). The spreading of the advancing liquid front was recorded using a high-speed motion analysis system (Kodak, series SR) with a digital camera able to take up to 1000 frames per second for up to 1 h.

The spreading of receding liquid fronts was analyzed by placing a thin foil of the alloy on top of the Mo substrate. The assembly was heated to the test temperature under the same conditions described above, and the receding spreading front was recorded using the high-speed video system.

After the experiments, the samples were analyzed using optical and scanning electron microscopy (SEM), as well as Auger electron spectroscopy. Cross sections were polished with 1 μm diamond and analyzed using optical microscopy and SEM-EDS.

Results and discussion

The first step in the analysis of high temperature spreading should be comparison with well-established models of low temperature systems. The goal is to determine the physicochemical processes that control spreading of high temperature liquids and identify the phenomena for which new models are required in order to develop theories that better describe the spreading of molten metals and oxides.

Spreading in low temperature systems (those in which the experimental temperature is low compared to the melting point of the substrate, typically $<(0.2–0.5)T_m^s$, T_m^s being the substrate melting point) is usually analyzed in terms of one fluid displacing another over a solid surface presumed to be effectively rigid and insoluble (regime I), where successive spreading regimes correspond to increasing degrees of concurrent substrate deformation [8]. Under these conditions, the capillary forces drive a homogeneous liquid toward a shape of constant curvature and the contact angle toward the θ_{1D} value given by the Young-Dupré equation:

$$\gamma_{lv} \cos\theta_{1D} = \gamma_{sv} - \gamma_{sl} \quad , \qquad (1)$$

where γ_{lv} and γ_{sv} are the liquid and solid surface energies, and γ_{sl} is the solid/liquid interfacial energy. Other driving forces from hydrostatic pressure gradients can be ignored here.

The theoretical analysis of spreading has focused on the search for a relationship between the dynamic contact angle θ_D and the dimensionless capillary number *Ca* [9]:

$$Ca = \frac{\eta v}{\gamma_{lv}} \quad , \qquad (2)$$

where η is the liquid viscosity and *v* is the spreading velocity, which, for the spontaneous spreading of a small drop, is equivalent to *dR/dt* (*R* is the drop radius). These relationships are usually tested under varied configurations, in which a liquid front moves over a solid substrate, displacing another fluid (gas or liquid). Configurations range from the spontaneous spreading of a liquid drop, to the forced spreading of liquids through capillaries, or the immersion or removal of solid rods or plates from liquid tanks, among others.

For low temperature systems, dynamic wetting has been analyzed from the perspectives of both continuum mechanics (hydrodynamics) and microscopic or molecular mechanisms [9-14]. The hydrodynamic analyses presume that the main force retarding spreading is viscous impedance. A popular expression for the relationship between contact angle and spreading velocity is the generalized Hoffman-Voinov-Tanner law, valid if *Ca* is small and the dynamic contact angle is lower than 3π/4 rads: [9, 10, 14]

$$Ca = \frac{1}{9 \cdot \mathrm{Ln}\left(\frac{L}{L_s}\right)} \left(\theta_D^3 - \theta_{1D}^3\right) \quad , \qquad (3)$$

where L is a characteristic capillary length, and L_s is the slip length; L_s corresponds to a thickness of the meniscus immediately adjacent to the solid wall over which the "no-slip" boundary condition of classical hydrodynamics is relaxed.

Microscopic analyses attribute the mechanisms controlling spreading to atomic dynamics at the triple line. Using an adsorption-desorption mechanism in which molecules of the advancing fluid displace those of the receding one at adsorption sites on the solid surface, Blake and Haynes developed an expression that can be used to describe the behavior of many low-temperature systems [11, 12]:

$$Ca = \frac{2\eta\lambda K_{\omega}}{\gamma_{lv}}\left[\sinh\left(\frac{\lambda^2\gamma_{lv}}{2kT}\left(\cos(\theta_0)-\cos(\theta_D)\right)\right)\right] \qquad (4)$$

$$K_{\varpi} = \left(\frac{kT}{h}\right)e^{\frac{-\Delta G_W}{NkT}} \quad , \qquad (5)$$

where n is the number of adsorption sites per substrate area, λ is their average spacing, k and h are Boltzmann's and Plank's constants, respectively, T is temperature, and N is Avogadro's number. The activation free energy for wetting ΔG_W derives mainly from the solid-fluid interaction. This is the energy barrier for the process required to replace one molecule of the receding fluid from the attachment site on the solid with one from the advancing fluid.

Similarly, some empirical relationships have been developed for the spontaneous spreading of small liquid drops. For systems with complete wetting, Marmur and Lelah found that most data can be fit using a simple power law [15]:

$$\pi R^2 = kt^{2n} \quad . \qquad (6)$$

For most of the data, $0.1 \leq n \leq 0.14$. For small droplets that retain constant curvature and completely wet the solid and for which $\theta_D << \pi/2$, the following relationship has also been proposed [16, 17]:

$$\frac{dR}{dt} \sim \theta_D^{(1-n)/3n} \quad . \qquad (7)$$

For n = 1/10, this equation is consistent with the Hoffman-Voinov-Tanner law

In contrast to what has been observed and modeled for low-temperature spreading, there is no unique angle-velocity relationship in the Ag-Mo system (Figure 3). Spreading times differing over four orders of magnitude have been recorded using almost identical experimental conditions (Figure 3). This behavior is similar for both Ag and Ag-Mo liquids.

It is not always possible to obtain good empirical power fittings (Eq. 6) to our experimental results. Additionally, the resulting values of n ~ 0.02–0.05 are smaller than those reported by Marmur and Lelah [15]. Furthermore, only the fastest spreading rates could be satisfactorily fitted using the models developed for low temperature systems (Eqs. 3 and 4).

The wide variability in the recorded spreading velocities points out the possibility that spreading in the Ag-Mo system is controlled in many cases by the movement of triple line ridges. It has been proposed that when the spreading temperatures are ≥ (0.2–0.5)T_m^s, the formation and movement of ridges at the triple junction controls spreading [5, 8, 18]. The ridges grow through local diffusion or solution/precipitation of the solid atoms in order to attain complete two-dimensional equilibrium of the interfacial forces at the triple line. The triple junction will remain attached to the ridge unless a sudden perturbation drives the macroscopic contact angle outside a stability range that depends on the ridge orientation, causing the wetting front to break away. One of the consequences of ridge-controlled spreading is that there is no unique wetting velocity for each dynamic contact angle, but rather a broad range of velocities that depend inversely on the ridge height, which in turn depends on the dynamic contact angle and the size of the perturbation that originated it. This will result in a wide variability in spreading velocities, as observed in the Ag-Mo system, where only the fastest velocities recorded could correspond to one-dimensional spreading on a flat substrate. It should be noted that when ridge evolution is controlled by interfacial diffusion, if there is no initial perturbation to nucleate the formation of a ridge, a condition exists wherein a liquid can spread on a flat surface quickly enough to suppress initiation of ridge growth even in the range of angles of stable ridge growth [5]. Diffusional fluxes are limited by the actual atomic jump frequency as the ridge height goes to zero. Consequently, a spreading velocity exists beyond which ridge formation is impossible even inside the stability range, because the jump frequency becomes too slow compared to the spreading velocity

and the first atomic-sized ridge cannot form at the triple junction. This critical velocity v_{cr} can be estimated as:

$$v_{cr} = \frac{6D_{sl}}{a} \quad , \tag{8}$$

where a is a jump distance and D_{sl} is the diffusion coefficient at the solid/liquid interface. Using the surface diffusion coefficients reported for molybdenum as a guide (~$4 \cdot 10^{-16}$ at 1000°C) [19] and $a \approx 1$ nm, the critical velocity v_{ca} should be on the order of ~ $2–3 \cdot 10^{-6}$. This critical velocity is several orders of magnitude lower than the velocities recorded in the experiments reported in this paper. It is expected that if the liquid front does not find a perturbation that will originate a ridge, it can spread on the flat surface in a fashion similar to that observed for low-temperature systems. This situation will correspond to the fastest spreading velocities recorded, which are on the order of, or even faster than, those observed for low temperature liquids of similar viscosity. It should be noted that, because liquid metals typically have surface energies one to two orders of magnitude above those of organic liquids, the hydrodynamic analysis predicts that for a similar driving force ($\theta_D^3 - \theta_{1D}^3$), metals should spread faster. All the slower spreading rates will correspond to cases in which a scratch or other topographic irregularity on the substrate surface nucleated a ridge at the triple line, so that spreading is controlled by the movement of that ridge or by a succession of breakaways and new ridge nucleation.

If the fastest kinetics corresponds to spreading on a flat surface, the data can be compared with the models developed for low temperature systems. Both the hydrodynamic and molecular-kinetics equations reproduce the results for the fastest spreading experiments well (Figure 4). However, using reasonable values for the liquid viscosity and surface

energy ($\eta \approx 0.004$ N·s·m^{-2} $\gamma_{lv} \approx 0.9$ J·m^{-2} [20]) the hydrodynamic fitting of our results implies a value of $L_s \approx 0$, which contradicts most hydrodynamic analyses of low-temperature data for which the slip length has microscopic but measurable dimensions (typically between 0.001 and 1 μm) [9, 21, 22]. The values of L_s derived from our experiments are not consistent with the continuum description of spreading. The parameters deduced from the molecular-kinetic analysis are more reasonable. The calculated distances between adsorption sites (0.1–1.0 nm) are, as expected, on the order of atomic distances. The calculated wetting activation energies are ~100 kJ, and the frequencies K_ω are around 10^8 s^{-1}, which are in the range of those reported for low temperature liquids (typically from 10^3 to 10^{10} s^{-1}) [11, 21]. The values calculated from the experiments reported in this paper are at the top of that range. The metal-metal interactions at the metastable interfaces that form during spreading are stronger than the Van der Walls type of forces mostly present for low-temperature systems. Stronger solid-liquid interactions should translate into less atomic mobility for the liquid atoms attached to the interfaces and smaller frequencies for the movement in the direction parallel to the substrate surface[10]. However, the calculated values are at the top of the range, suggesting that the rate-determining step is not the movement of one atom from one site to another on the surface of the solid, but the movement of an atom from the liquid onto a site on the solid surface.

In many practical situations for low and high temperature spreading, it has been observed that advancing and receding liquid fronts arrive at different stationary contact angles. This wetting hysteresis is usually attributed to morphological or chemical

inhomogeneities in the substrate, or to the fact that for contact angles close to equilibrium, spreading occurs too slowly to be accurately recorded in practical experiments. Another source of hysteresis can be nonequilibrium adsorption. The equilibrium interfacial tensions describe actual forces only when spreading is so slow that all interfaces always have equilibrium levels of adsorbate. When spreading is too fast, several nonequilibrium situations can occur. For example, when the primary source of adsorbate for the solid surface is the liquid itself (solvent or solute), spreading can be too rapid to reach equilibrium levels on the surface ahead of the liquid. In the *dry spreading* limit, a drop can spread to very low or vanishing contact angles because the surface directly ahead is free of any adsorbate; as a consequence, the energy for a clean surface γ_{sv}^{o} ($\gamma_{sv}^{o} \geq \gamma_{sv}$) should be used when defining the wetting driving forces (Eq. 1) in combination with equilibrium interface and liquid energies [17]. In contrast, a receding drop would tend to leave the adsorbate already established under the liquid. Leaving too much adsorbate would effectively decrease the solid surface energy, promoting retraction.

Even though some degree of hysteresis has been observed in the Ag-Mo system (Figure 5), for some experiments advancing and receding drops reach a common contact angle of ~35° for pure silver and ~37° for the Ag-Mo alloy (Figure 5). This agrees with the idea that for these experiments, spreading occurs on a flat substrate without ridging formation (regime I) or that the ridge is very small compared to the radius of curvature for the liquid, $h/R << 0.1$, and can be carried by a moving front (regime II) [8]. In both situations, the capillary forces drive the macroscopic contact angle toward a value very

near that satisfying Young's equation. In some experiments advanced liquid fronts stop at relatively high angles (Figure 5). This will correspond to a situation in which a large ridge or a scratch pins the triple line stopping spreading. In the drop-transfer experiments, nonequilibrium adsorption does not seem to affect the final contact angles. Even though Auger electron spectroscopy has shown the existence of adsorbed Ag on the free Mo surface ahead of the drop after the experiments (Figure 6), no noticeable differences in the relative height of the Mo and Ag peaks can be observed between advancing and receding experiments with Ag or Ag-Mo liquids.

Liquid silver and molybdenum are not in equilibrium, since there is some finite solubility of Mo in Ag at 1000°C. However, an interfacial energy can be associated with the metastable interface between pure silver and molybdenum. This can be better understood by doing a mental cleavage experiment in which that interface is separated without any dissipation. The work performed (it can be named work of separation W_S, as opposed to the thermodynamic equilibrium work of adhesion W_{ad}) [23] is:

$$W_S = \gamma_{Ag} + \gamma_{Mo} + \gamma^0_{Ag-Mo} \quad , \qquad (9)$$

where γ_{Ag} and γ_{Mo} are the surface energies of pure silver and molybdenum, and γ^0_{Ag-Mo} is the interfacial energy associated with the metastable interface. After spreading, no appreciable diffusion of Mo into the liquid silver could be detected using SEM-EDS (Figure 7). The solubility of silver in solid Mo at 1000°C is very low (<0.00578 at%) [7]. The results from our wetting experiments indicate that the interfacial energy associated

with the "metastable" interface (γ^0_{Ag-Mo}) is very similar to the equilibrium γ_{sl} between the Ag-Mo liquid and the Mo substrate, as can be expected from the low mutual solubility [24]. Using reasonable values for the surface energies ($\gamma_{Ag} \sim 0.9$ J·m^{-2} and $\gamma_{Mo} \sim 2.6$ J·m^{-2}) [20] and the measured common contact angles reached by advancing and receding drops, $\gamma^0_{Ag-Mo} \approx \gamma_{Ag\text{-}Mo} \approx 1.8\text{-}1.9$ J·m^{-2} (the effect of Mo dissolution on the surface energy of silver has been disregarded).

Conclusion

A wide range of spreading rates has been recorded during the wetting of Ag and Ag-Mo liquids on Mo substrates, suggesting that spreading is controlled by the movement of triple line ridges. Only the fastest spreading rates are consistent with a liquid front moving on a flat surface and can thus be analyzed using a molecular-kinetic model. Even though silver adsorption has been observed ahead of the drop on the free Mo surface, there is no evidence of nonequilibrium adsorption. Pure silver and silver-molybdenum alloys reach similar equilibrium contact angles, which would indicate very similar interfacial energies, as can be expected from the low mutual solubilities.

Acknowledgements

This work was supported by the Director, Office of Science, Office of Basic Energy Sciences, Division of Materials Sciences and Engineering, of the U.S. Department of Energy under Contract No. DE-AC03-76SF00098. This work was in part supported by

NEDO International Joint Research Grant supervised by the Ministry of Economy, Trade and Industry of Japan.

References

1. P. R. Chidambaram, A. Meier and G. R. Edwards: Mater. Sci. Eng. a-Struct. Mater. 206 (1996) 249-258.

2. N. Eustathopoulos, M. Nicholas and B. Drevet: Wettability at High Temperatures, editors, Elsevier, Oxford (1999)

3. R. E. Loehman and A. P. Tomsia: J. Amer. Ceram. Soc. 77 (1994) 271-274.

4. R. E. Loehman, A. P. Tomsia, J. A. Pask and S. M. Johnson: J. Amer. Ceram. Soc. 73 (1990) 552-558.

5. E. Saiz, R. M. Cannon and A. P. Tomsia: Oil Gas Sci. Technol. 56 (2001) 89-96.

6. J. C. Ambrose, M. G. Nicholas and A. M. Stoneham: Act. Met. Mat. 40 (1992) 2483-2488.

7. T. B. Massalski and ASM International.: Binary alloy phase diagrams, editors, ASM International, Materials Park, Ohio (1990)

8. E. Saiz, A. P. Tomsia and R. M. Cannon: Acta. Mater. 46 (1998) 2349-2361.

9. S. F. Kistler. Hydrodynamics of wetting. In: J. C. Berg, J. C. Bergs. Wettability. Marcel Dekker Inc, New York (1993) 311-429.

10. M. J. de Ruijter, T. D. Blake and J. De Coninck: Langmuir 15 (1999) 7836-7847.

11. T. D. Blake. Dynamic contact angles and wetting kinetics. In: J. C. Berg, J. C. Bergs. Wettability. Marcel Dekker Inc., New York (1993) 251-309.

12. T. D. Blake and J. M. Haynes: J. Colloid. Interfac. Sci. 29 (1969) 174.

13. P. G. Petrov and J. G. Petrov: Langmuir 8 (1992) 1762-1767.

14. O. V. Voinov: Izv. Akad. Nauk SSSR Mekh. Zhidk. Gaza (USSR) (1976) 76-84.

15. M. D. Lelah and A. Marmur: J. Colloid. Interfac. Sci. (USA) 82 (1981) 518-25.

16. L. H. Tanner: J. Phys. D, Appl. Phys. (UK) 12 (1979) 1473-84.

17. P. G. de Gennes: Rev. Mod. Phys. (USA) 57 (1985) 827-63.

18. E. Saiz, A. P. Tomsia and R. M. Cannon: Scripta Mater. 44 (2001) 159-164.

19. N. A. Gjostein. Surface Self-Diffusion. In: Metal Surfaces. American Society for Metals, Metals Park, Ohio (1963) 99-154.

20. C. J. Smithells and E. A. Brandes: Metals Reference Book, Butterworths, London ; Boston (1976)

21. M. Schneemilch, R. A. Hayes, J. G. Petrov and J. Ralston: Langmuir 14 (1998) 7047-7051.

22. R. G. Cox: J. Fluid. Mech. (UK) 168 (1986) 169-94.

23. A. P. Tomsia, E. Saiz, B. J. Dalgleish and R. M. Cannon. Wetting and strength issues in ceramic/metal bonding. In proceedings of the 4th Japan International SAMPE Symposium & Exposition (JISSE-4) Tokyo, Japan: 1995.

24. P. Gumbsch and M. S. Daw: Phys. Rev. B-Condensed. Matter. 44 (1991) 3934-3938.

Figure Captions

Figure 1. Schematic of the Ag-Mo binary system, showing the liquids used for these wetting experiments (after reference [7]). The Ag-Mo liquid is saturated with molybdenum at the experimental temperature. The solubility of silver in solid Mo is lower than 0.00578 at%.[7]

Figure 2. Schematic of the drop-transfer setup.

Figure 3. Variation of contact angle and drop radius with time during the spreading of silver drops on molybdenum substrates. Data for two different experiments (squares and circles) are shown. As can be observed, spreading times can vary as much as four to five orders of magnitude under similar experimental conditions. Intermediate spreading kinetics has also been observed.

Figure 4. Fitting of the spreading of liquid Ag on Mo to hydrodynamic and molecular-kinetic models. Data from different experiments is plotted. The fittings are performed in the range of validity of the hydrodynamical model (contact angles below $3\pi/4$).

Figure 5. Final contact angles reached by advancing and receding Ag and Ag-Mo drops on Mo substrates. Even though some variability exists and in some cases advancing fronts stop at higher values, in many experiments a common contact angle is reached after the advancing and receding experiments.

Figure 6. Scanning electron microscopy and associated Auger electron spectroscopy of the free surface of molybdenum after the spreading of an Ag-Mo drop at 1000°C for 10 seconds.

Figure 7. SEM micrograph and associated EDS line analysis of the interface between Ag and Mo after one hour at 1000°C. No interdiffusion could be observed.

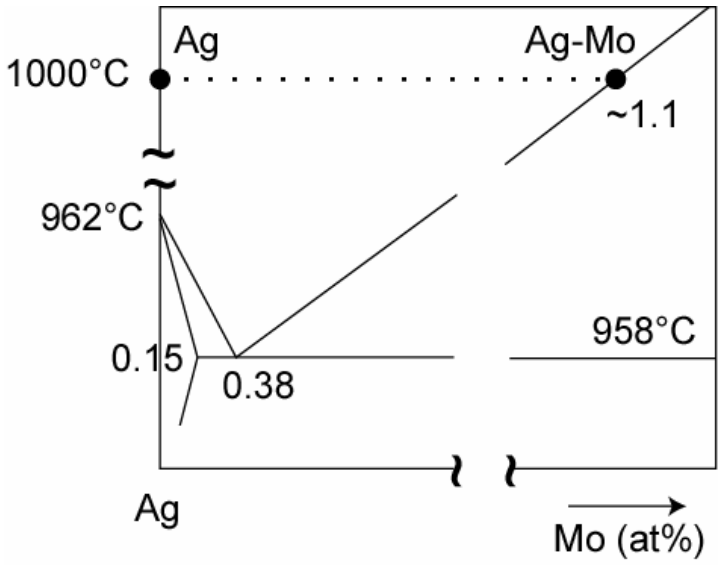

Figure 1

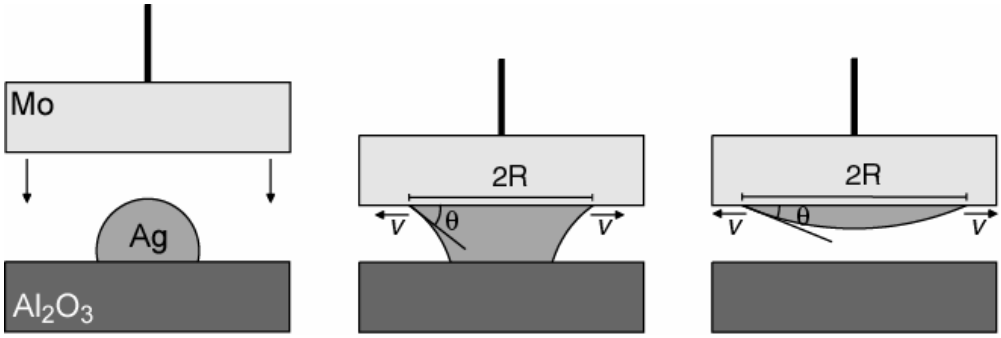

Figure 2

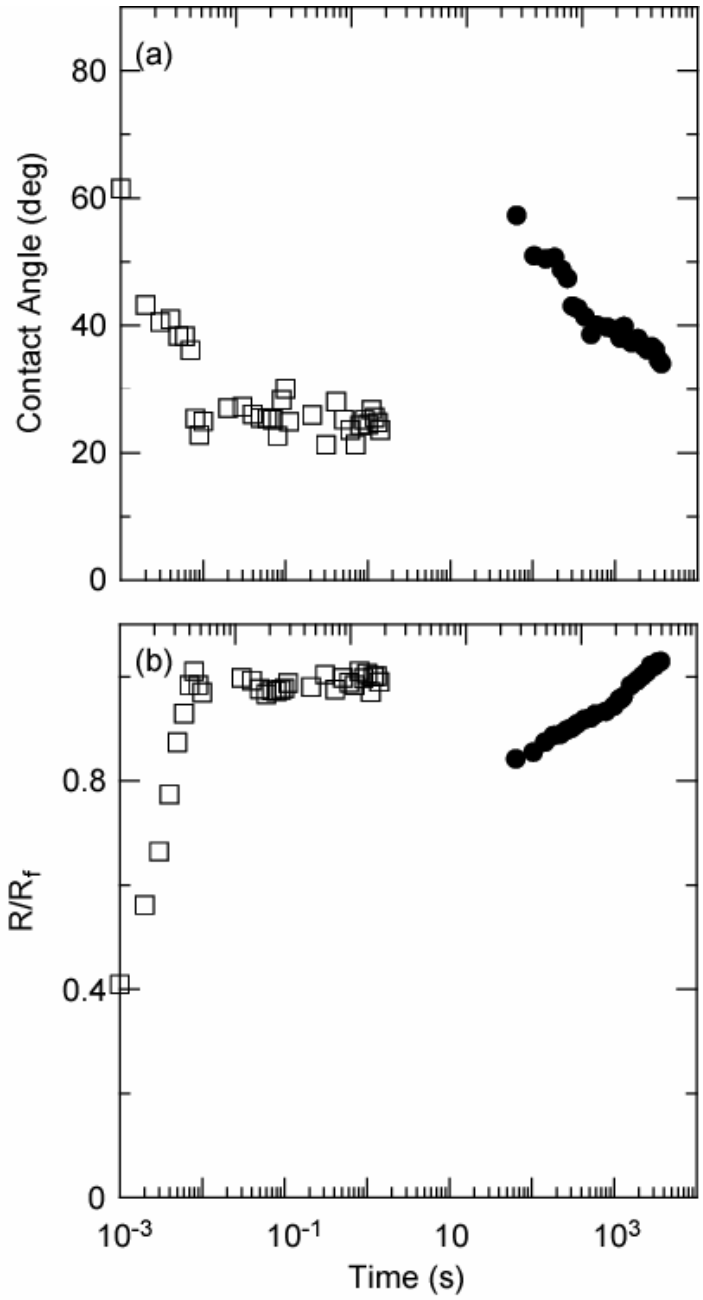
(a)
80
60
40
20
0
Contact Angle (deg)
(b)
0.8
0.4
0
R/R_f
10^-3
10^-1
10
10^3
Time (s)

Figure 3

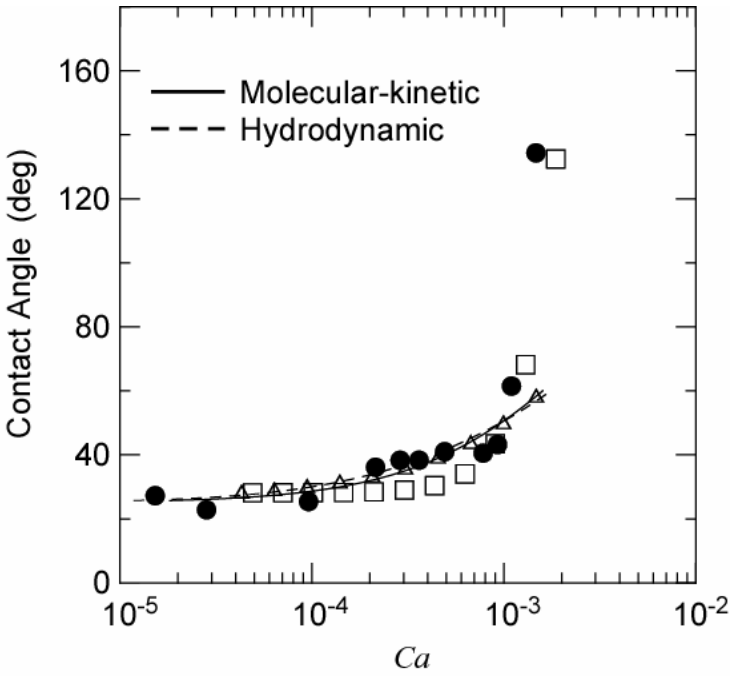

Figure 4

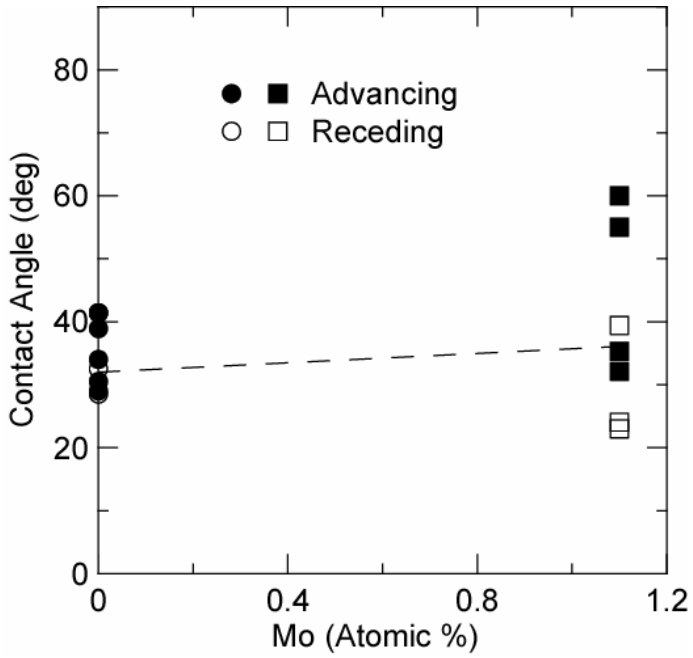

Figure 5

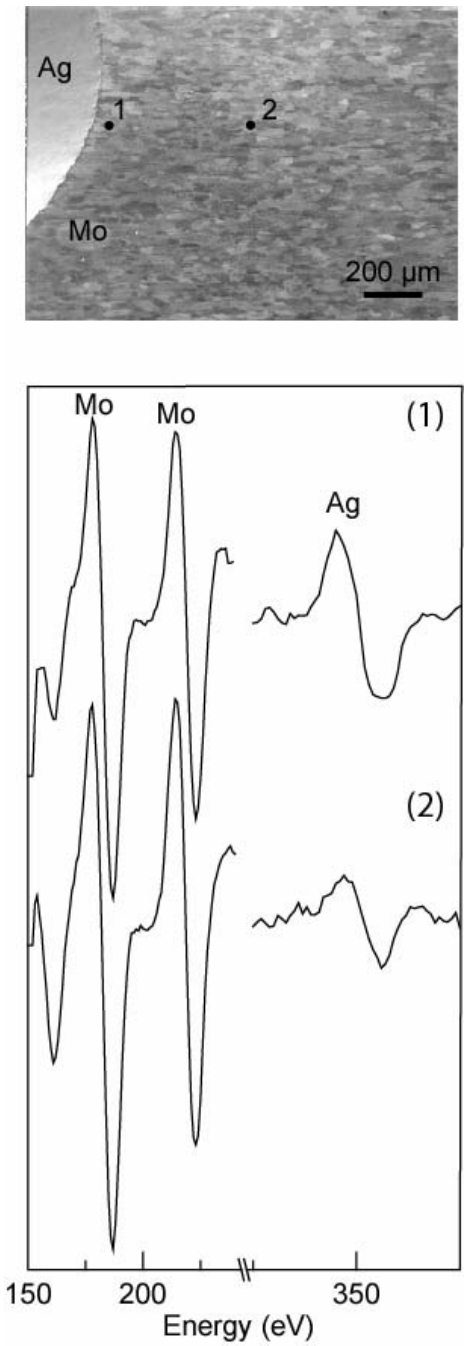

Figure 6

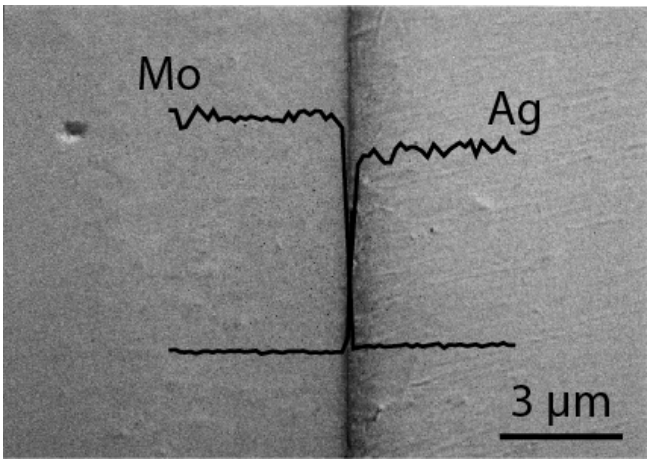

Figure 7